Electronic structure of a monoatomic Cu_2Si layer on a Si(111) substrate

M. Cameau,[1,2] R. Yukawa,[3] C.-H. Chen,[4] A. Huang,[4] S. Ito,[5] R. Ishibiki,[6] K. Horiba,[3] Y. Obata,[3] T. Kondo,[7,6] H. Kumigashira,[3] H.-T. Jeng,[4,8,9] M. D'angelo,[2] and I. Matsuda[5,*]

[1]*Sorbonne Université, Institut de Minéralogie, de Physique des Matériaux et de Cosmochimie (IMPMC), F-75005 Paris, France*
[2]*Sorbonne Université, Institut des NanoSciences de Paris (INSP), F-75005 Paris, France*
[3]*Institute of Materials Structure Science, High Energy Accelerator Research Organization (KEK), Tsukuba, Ibaraki 305-0801, Japan*
[4]*Department of Physics, National Tsing Hua University, Hsinchu 30013, Taiwan*
[5]*Institute for Solid State Physics, The University of Tokyo, Kashiwa, Chiba 277-8581, Japan*
[6]*Faculty of Pure and Applied Sciences, University of Tsukuba, Tsukuba 305-8571, Japan*
[7]*Materials Research Center for Element Strategy, Tokyo Institute of Technology, Yokohama 226-8503, Japan*
[8]*Physics Division, National Center for Theoretical Sciences, Hsinchu 30013, Taiwan*
[9]*Institute of Physics, Academia Sinica, Taipei 11529, Taiwan*

(Received 31 October 2018; published 24 April 2019)

Fermi surfaces and band dispersion curves of a Cu_2Si layer on Si(111), quasi-"5×5" were mapped by angle-resolved photoemission spectroscopy using synchrotron radiation. Two metallic bands were observed within the Si bulk band gap, which are likely assigned to the electronic bands of the Cu_2Si layer. Additional bands were found in the Si bulk band gap that originate from the interactions between the substrate state and the Cu_2Si states that have the p_z character. The present research aims at investigating the changes in the electronic structure of an atomic layer when prepared on a substrate.

DOI: 10.1103/PhysRevMaterials.3.044004

I. INTRODUCTION

Atomic layers have been significant playgrounds for low-dimensional physics. These systems have recently attracted both academic and technological interest due to observations and predictions of Dirac electrons. The mastery of Dirac electrons could lead to high-frequency and low-dissipation devices for electronic applications and be the next revolution in materials science. Dirac cones have been measured experimentally in layers of graphene [1,2] and have also been predicted for *X*enes such as silicene [3–5], germanene [6,7], phosphorene [8–10], bismuthene [11,12], borophene [13–15], antimonene [16,17], and stanene [18,19]. Layers of *X*ene have been prepared on solid surfaces; however, the observed electronic states were different from the predictions for freestanding layers. Instead of a single Dirac cone at the *K* point, pairs of Dirac cones are observed in layers of silicene or borophene on the Ag(111) substrates [4,14,15]. In contrast to the topological insulating nature expected for stanene, the layer grown on a Bi_2Te_3 substrate exhibits a metallic band at the Γ point [18]. While these experimental facts leave space for controlling electronic states of atomic layers prepared on substrates, much more evidence is required to understand the evolution of their electronic states.

In the present research we focus on the Cu_2Si layer, which has been predicted to host Dirac nodal fermions in its freestanding form and it was experimentally demonstrated to host them when prepared on a Cu(111) substrate [22]. Aiming at finding a suitable nonconducting substrate, which would represent a huge leap towards practical applications, we prepared the Cu_2Si layer on a Si(111) substrate. On the (111) crystal surface of the well-known semiconducting Si substrate, the Cu_2Si quasi-"5×5" surface reconstruction has been known to be obtained by Cu deposition [20,23,24], as shown in Fig. 1 by low-energy electron diffraction (LEED). The surface is "discommensurate" (incommensurate) with the substrate lattice, resulting in a quasi-"5×5" periodicity. The structure model, proposed by Zegenhagen *et al*. [20,21], has been widely accepted and was also confirmed recently [25]. As shown in Fig. 2, it consists of a surface tiled with the Cu_2Si quasi-"5×5" domains, lacking the long-range order of the Cu_2Si monolayer. The atomic structure of the Cu_2Si layer can be considered as replacement of upper Si atoms in the Si(111) topmost layer with the Cu atoms of the honeycomb lattice, as shown in Fig. 2. It is of note that, in the discommensurate phase, the degree of local Si-Si back-bonding depends on the individual sites, as presented in Fig. 2.

In the present research, we prepared the Si(111)quasi-"5×5" Cu surface and studied its electronic band structure by band-mappings with angle-resolved photoemission spectroscopy (ARPES) and by band calculations with density functional theory (DFT). Two partially occupied or metallic bands and fully occupied bands of the surface states were observed within the Si bulk band gap. These states likely originate from three electronic states of the Cu_2Si layer, evidencing the effect of interactions between the layer and the substrate.

II. EXPERIMENTAL SECTION

The experiments were conducted at the beamline BL-2A MUSASHI of Photon Factory, KEK, Japan. Measurements of angle-resolved photoemission spectroscopy were performed

*imatsuda@issp.u-tokyo.ac.jp

FIG. 1. LEED image of the Cu_2Si quasi-"5 × 5" surface reconstruction taken at normal incidence. Electron energy is 46 eV. The white arrow indicates one of the fundamental Si(111)1×1 spots.

at 20 K. The samples were prepared *in situ* in a ultrahigh vacuum (UHV) chamber. Clean Si(111) surfaces with a 7 × 7 reconstruction were prepared by flashing at 1200 °C, followed by annealing at 850 °C. A Si wafer of *n* type (<0.02 Ω cm) was used. The Cu_2Si layer was prepared by Cu deposition on the Si(111) 7 × 7 at 630 °C. A Cu evaporator was prepared using a tungsten filament and a copper wire (99.999% purity). At a Cu coverage of 1 monolayer (ML), as determined by a quartz balance, a quasi-"5×5" phase was confirmed by sharp LEED patterns, as shown in Fig. 1. This discommensurate surface reconstruction is in total agreement with anterior studies on this material [20,21,23,25].

First-principles calculations were performed using the projected augmented wave method (PAW) [26,27] as implemented in the Vienna Ab initio Simulation Package (VASP) [28–31] based on density functional theory with the Perdew-Burke-Ernzerhof (PBE) type of generalized gradient approximation (GGA) and GGA plus Hubbard U (PBE+U) scheme. The 12 × 12 × 1 Monkhorst-Pack k mesh and a cutoff energy of 400 eV are used in the self-consistent field calculations. The on-site Coulomb energy $U = 7.0$ eV [32] is adopted for Cu atoms in the PBE+U calculations. The geometries of all the systems are optimized with the total energies converged within 10^{-4} eV. To study the substrate effect in the Cu_2Si/Si(111) systems, we put a Cu_2Si 1 × 1 monolayer on top of a 12-layer Si 1 × 1 substrate with a Cu_2Si lattice constant of 4.09 Å.

III. RESULTS AND DISCUSSION

Figure 3(a) shows the photoemission Fermi surface map of the Cu_2Si surface, taken at a photon energy of 70 eV and with linear-horizontal (LH) polarization. These parameters were experimentally determined as the optimal ones for a high resolution of the electronic bands. The observation of the Fermi surface clearly indicates that the surface is metallic. Contours of the Fermi surface are composed of a hexagon, exhibiting large photoemission intensity and fine intensity structures. The photoemission bands are composed of the original band and those coming from umklapp scattering associated with the quasi-"5×5" periodicity. The map of the

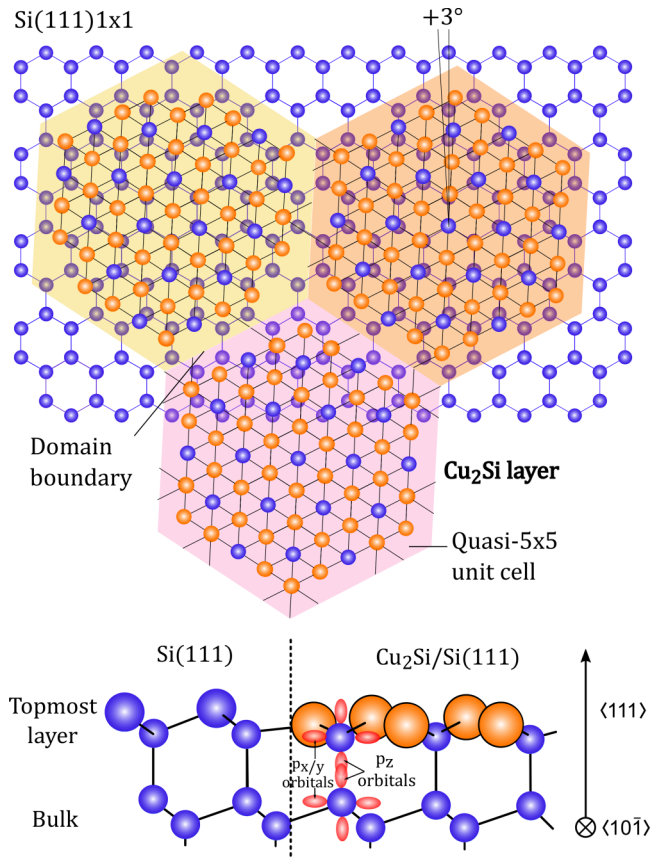

FIG. 2. (a) Schematic representation of the discommensurate Cu_2Si/Si(111) quasi-"5×5" layer as described by Zegenhagen *et al.* [20,21]. Copper atoms are represented by orange spheres, silicon atoms by blue spheres. The Cu_2Si layer replaces the topmost layer of Si(111)-1 × 1 surface. The lattice parameter of this topmost Cu_2Si layer is larger by 9.7% compared to the Si(111), and the large lattice misfit leads to a regular dislocation network, creating discommensurate domains, represented here by the large hexagons of variable colors. Complete tiling of the surface requires three types of twisted domains (±3° with respect to the substrate orientation), two of them being rotationally equivalent (here the pink and orange hexagon). (b) Side view. The left-hand side of the surface shows clean Si(111), while the right-hand part is covered with Cu (orange sphere), showing the positioning of the Cu_2Si layer.

Fermi surface is reproduced by taking into account two types of Fermi surfaces (hexagonal and flower-shaped) with a ±3° rotations and by tiling with the umklapp-scattering vectors, as shown in Figs. 3(b)– 3(d). It is of note that the hexagonal and flower-shaped Fermi surfaces match with the energy contours of the α and β bands of the Cu_2Si layer [22,33]. The tiling of the hexagonal (α) band is consistent with the previous band-mapping of the Si(111)quasi-"5×5"-Cu surface [24].

The electronic band structure was measured along two directions in the reciprocal space: $\overline{\Gamma}$-$\overline{M}$ and $\overline{\Gamma}$-$\overline{K}$ of the Si(111) 1 × 1 Brillouin zone surface. The results are shown in Figs. 4 and 5. Starting with Fig. 4, one can recognize the silicon bulk bands [34] at the $\overline{\Gamma}$ point. The bulk bands are composed of many subbands that are generated due to the quantum confinement by the narrow space-charge layer [35]. The white dotted line in the figure traces the edge of the bulk bands and,

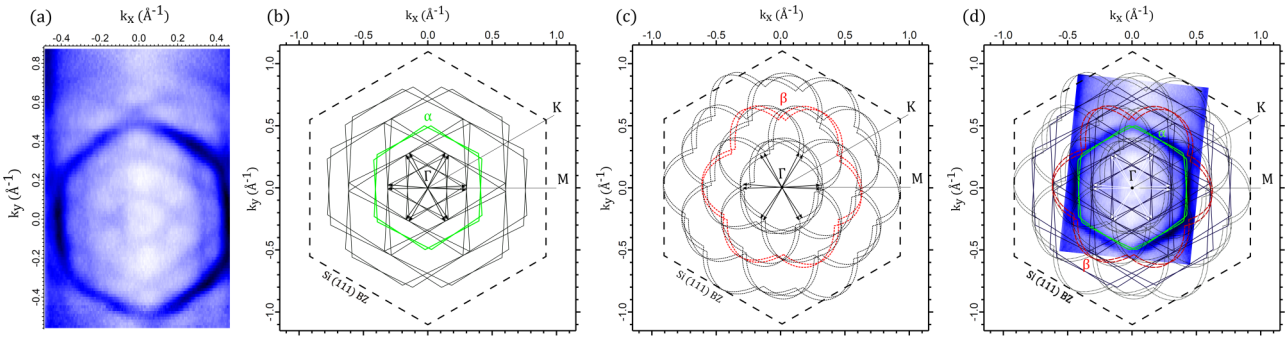

FIG. 3. Study of the Fermi surface of Cu_2Si. (a) Constant energy contour map measured using 70-eV linear horizontal polarized photons at the Fermi level. Two bands, one hexagonal (α) and one flower-shaped (β), are observed, as well as lighter patterns arising from umklapp scattering. (b) Schematic representation of the hexagonal α band, in green, and its umklapp tiling, in black. The umklapp vectors, by which the α band is translated, are represented by the arrows centered on Γ, and the Si(111) Brillouin zone is represented by the dashed hexagon. (c) Schematic representation of the flower-shaped β band, in red, and its umklapp tiling, in black. (d) Superposition of (a), (b), and (c), creating the complete quasi-"5×5" umklapp scattering of the Fermi surface.

within the bulk band gap, one can identify dispersion curves of the α band that crosses the Fermi level (E_F). The Fermi vector along the $\overline{\Gamma}$-$\overline{M}$ direction is 0.42 Å^{-1}, which is similar to the previously reported value [24]. The metallic β band, fainter, is also identified. Other bands, indicated by arrows in the figure, correspond to replica bands by the quasi-"5×5" umklapp scattering [24].

Along the $\overline{\Gamma}$-$\overline{K}$ direction (Fig. 5), one can clearly observe the two metallic bands, α and β, that cross the Fermi level. The Fermi vectors along the $\overline{\Gamma}$-$\overline{K}$ direction are estimated to be 0.48 and 0.54 Å^{-1} for the α and β bands, respectively. It is of note that previous research on Si(111) [24] reported one of the bands, α. In the figure, one can also find replica bands of the quasi-"5×5" umklapp scattering [24]. We confirm observation of no other band at the Fermi level for different photon energies (hν = 35, 40, 50, 60, 80, 100 and 105 eV), which are not shown here.

The α and β bands observed in the present research are hole pockets and also have similar dispersion curves (Fermi surfaces) to those of the α_+ and β_+ bands in Ref. [22]. Thus, it is natural to consider that origins of the α and β states are α_+ and β_+ of the freestanding layer, respectively. A comparison between Fermi vectors for three different systems is presented in Table I. Taking parameters of the freestanding Cu_2Si as a reference, the wave vectors show opposite shifts between the Cu and Si substrates. The k_F values become smaller on Cu(111) but larger on Si(111), indicating a lower and higher shift in energy of the α and β bands, respectively.

Concerning the γ_- band in the freestanding Cu_2Si layer, it was not observed under the present experimental conditions at the Fermi level for the Si(111)quasi-"5×5"-Cu surface, which is sharply in contrast to behaviors of α and β bands. We infer that this difference is due to the orbital symmetry. According to the previous report [22], the α_+ and β_+ states have the mixed Si p_x/p_y and Cu p_x/p_y characters. On the other hand, the γ_- state has the Si p_z and Cu p_z character [22]. In the layer, the α_+ and β_+ states distribute in-plane, while the γ_- state extends out-of-plane. Thus, it is expected that the p_z states in the Cu_2Si layer make interactions with Si dangling-bond (p_z) states of the Si(111) substrate, resulting in formation of the bonding states. This picture is consistent with the structural model of the Si(111)quasi-"5×5"-Cu surface in

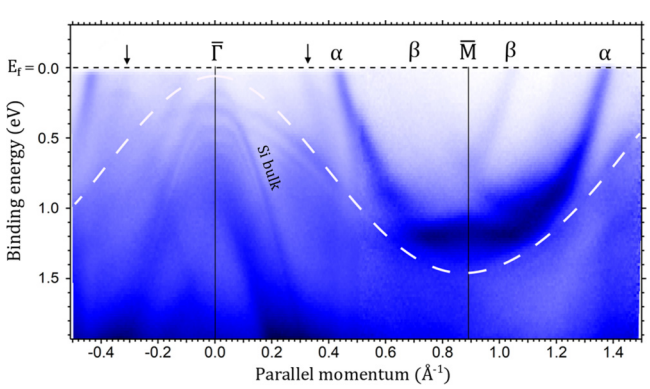

FIG. 4. Photoelectron dispersion plot of Cu_2Si monolayer on Si(111) substrate along the $\overline{\Gamma}$-$\overline{M}$ direction, using 70-eV LH-polarized photons. Silicon bulk bands are represented by a white dotted line. Above it, two metallic bands labeled as α and β, and the umklapp replica of the alpha band, denoted by an arrow, are visible.

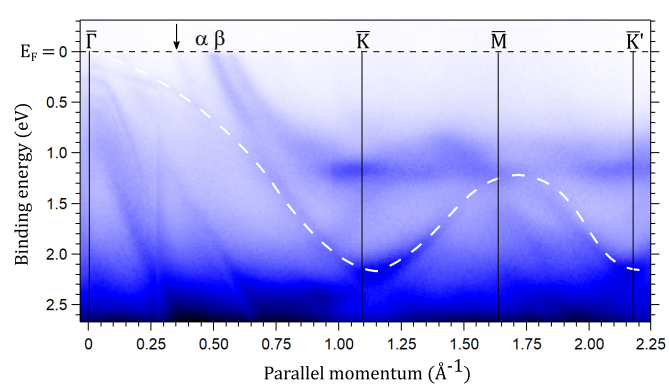

FIG. 5. Photoelectron dispersion plots of Cu_2Si monolayer on Si(111) substrate along the $\overline{\Gamma}$-$\overline{K}$ direction using 70-eV LH-polarized photons. The projected Si bulk states are represented by the white dotted line. Above it, two metallic bands, labeled as α and β, are visible, as well as an umklapp replica band of α denoted by an arrow.

TABLE I. Fermi vectors k_F in the three systems: freestanding Cu_2Si, $Cu_2Si/Cu(111)$, and $Cu_2Si/Si(111)$, for bands α and β, along the $\overline{\Gamma}$-$\overline{K}$ and $\overline{\Gamma}$-$\overline{M}$ directions. The unit is $Å^{-1}$. Values of the freestanding layer are obtained from the DFT calculation, while those of the $Cu_2Si/Cu(111)$ are supplied from the previous research [22]. For $Cu_2Si/Si(111)$, values are experimentally determined with accuracy of ± 0.02 $Å^{-1}$.

Direction	band	Freestanding Cu_2Si	Cu_2Si Cu(111)	Cu_2Si Si(111)
	α	0.37	0.23	0.48
$\overline{\Gamma}$-$\overline{K}$	β	0.39	0.27	0.54
	α	0.34	0.21	0.42
$\overline{\Gamma}$-$\overline{M}$	β	0.50	0.31	0.65

Fig. 2(b), underlining the bonding between the Si atoms from the surface and the bulk. As shown in Fig. 5, one can recognize electronic band at binding energy of 1–2 eV that are different from the α and β (replica) bands. Since the dispersion curves are located within the bulk band gap, the bands are assigned to the surface that are likely originated from the γ_- band. In order to confirm the picture, the DFT calculation was held on the $Cu_2Si/Si(111)$.

In Fig. 6, the calculated band structures of a Cu_2Si monolayer are presented for the freestanding layer and for the layer grown on a Si(111) substrate. For the freestanding Cu_2Si, Fig. 6(a), the band structure is consistent with the previous report [22]. Three metallic bands are labeled: two hole pockets, α_+ and β_+, and one electron pocket, γ_-, at the $\overline{\Gamma}$ point. The bands cross each other in regions with linear dispersion and generate two loops of the nodal lines [22]. Wave functions of the α_+ and β_+ bands have even parity, while that of the γ_- band has odd parity. On the Si substrate, we made calculation with the commensurate $Cu_2Si/Si(111)$ structure to model the Si(111)quasi-"5×5"-Cu surface. Despite the simplicity, the model is sufficient to capture electronic change coming from by the back-bond formation between the overlayer and the substrate. As shown in Fig. 6(b), the α and β bands remain almost unchanged while the γ band changes significantly. Furthermore, comparing Figs. 6(a) and 6(b), one recognizes additional bands around the K point at binding energy of 1–2 eV in (b), as expected in Fig. 5. The calculation supports our experimental results, evidencing that the γ band is much influenced than the α and β bands. It is of note that the calculation model reproduces only a part of the discommensurate phase. We leave open the possibility of the existence of the metallic freestanding-like γ band if there is a domain of the Cu_2Si layer on the surface that does not have local bonding with the substrate Si atoms.

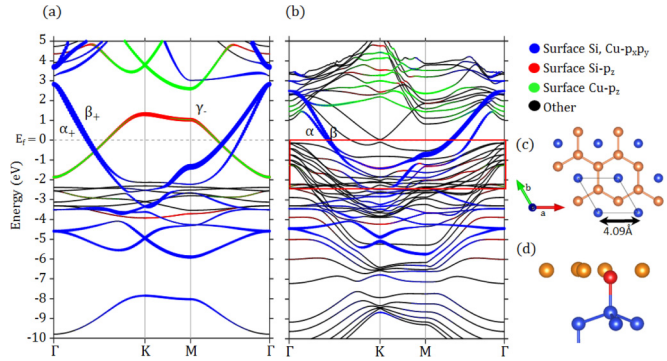

FIG. 6. Calculated band structure of a Cu_2Si monolayer. (a) Freestanding. Three metallic bands are clearly identified, namely, α_+, β_+, and γ_-. (b) On Cu_2Si on Si(111), following the model in (c, d). The contributions of the different orbitals are represented as follows: red from the surface Si-p_z, green from the surface Cu-p_z, blue from the surface Si and surface Cu p_x and p_y, and black for other sources. The red rectangle in (b) represents the extent of the ARPES experiment. (c) Top view of the Cu_2Si structure. (d) Side view of the $Cu_2Si/Si(111)$ structure, based on the model in Fig. 2, used for the DFT calculation.

IV. CONCLUSIONS

In summary, we mapped Fermi surfaces and band dispersion curves of a Cu_2Si layer on Si(111), with a quasi-"5×5" surface reconstruction, by angle-resolved photoemission spectroscopy and compared the result with the DFT band calculation. We found that electronic states with x-y (in-plane) character remained unchanged but those with z (out-of-plane) character are modified when the overlayer is prepared on a Si substrate. The present research demonstrates the electronic evolution of a monolayer in various environments, linking the theoretically predicted freestanding monolayer to the one prepared on a substrate.

ACKNOWLEDGMENTS

This work was supported by the Grant-in-Aid for Specially Promoted Research (KAKENHI 18H03874) from the Japan Society for the Promotion of Science, and by a grant from the Labex MATISSE. The preliminary experiment was performed at facilities of the Synchrotron Radiation Research Organization, the University of Tokyo. The computational work was supported by the Ministry of Science and Technology, Taiwan. H.T.J. also thanks the CQT-NTHU-MOE, NCHC, and CINC-NTU, Taiwan, for technical support. Baojie Feng is acknowledged for providing information on the $Cu_2Si/Cu(111)$ system.

[1] K. S. Novoselov, A. K. Geim, S. V. Morozov, D. Jiang, M. I. Katsnelson, I. V. Grigorieva, S. V. Dubonos, and A. A. Firsov, Two-dimensional gas of massless Dirac fermions in graphene, Nature (London) **438**, 197 (2005).

[2] Y. Zhang, Y.-W. Tan, H. L. Stormer, and P. Kim, Experimental observation of the quantum Hall effect and Berry's phase in graphene, Nature (London) **438**, 201 (2005).

[3] A. Fleurence, R. Friedlein, T. Ozaki, H. Kawai, Y. Wang, and Y. Yamada-Takamura, Experimental Evidence for Epitaxial Silicene on Diboride Thin Films, Phys. Rev. Lett. **108**, 245501 (2012).

[4] C.-L. Lin, R. Arafune, K. Kawahara, N. Tsukahara, E. Minamitani, Y. Kim, N. Takagi, and M. Kawai, Structure of silicene grown on Ag(111), Appl. Phys. Express **5**, 045802 (2012).

[5] S. Sadeddine, H. Enriquez, A. Bendounan, P. Kumar Das, I. Vobornik, A. Kara, A. J. Mayne, F. Sirotti, G. Dujardin, and H. Oughaddou, Compelling experimental evidence of a Dirac cone in the electronic structure of a 2D Silicon layer, Sci. Rep. **7**, 44400 (2017).

[6] M. E. Dávila, L. Xian, S. Cahangirov, A. Rubio, and G. Le Lay, Germanene: A novel two-dimensional germanium allotrope akin to graphene and silicene, New J. Phys. **16**, 095002 (2014).

[7] C.-H. Lin, A. Huang, W. W. Pai, W.-C. Chen, T.-Y. Chen, T.-R. Chang, R. Yukawa, C.-M. Cheng, C.-Y. Mou, I. Matsuda, T.-C. Chiang, H.-T. Jeng, and S.-J. Tang, Single-layer dual germanene phases on Ag(111), Phys. Rev. Mater. **2**, 024003 (2018).

[8] H. Liu, A. T. Neal, Z. Zhu, Z. Luo, X. Xu, D. Tománek, and P. D. Ye, Phosphorene: An unexplored 2D semiconductor with a high hole mobility, ACS Nano **8**, 4033 (2014).

[9] L. Li, Y. Yu, G. J. Ye, Q. Ge, X. Ou, H. Wu, D. Feng, X. H. Chen, and Y. Zhang, Black phosphorus field-effect transistors, Nat. Nanotechnol. **9**, 372 (2014).

[10] J. Kim, S. S. Baik, S. W. Jung, Y. Sohn, S. H. Ryu, H. J. Choi, B.-J. Yang, and K. S. Kim, Two-Dimensional Dirac Fermions Protected by Space-Time Inversion Symmetry in Black Phosphorus, Phys. Rev. Lett. **119**, 226801 (2017).

[11] T. Nagao, S. Yaginuma, M. Saito, T. Kogure, J. Sadowski, T. Ohno, S. Hasegawa, and T. Sakurai, Strong lateral growth and crystallization via two-dimensional allotropic transformation of semi-metal Bi film, Surf. Sci. **590**, 247 (2005).

[12] F. Reis, G. Li, L. Dudy, M. Bauernfeind, S. Glass, W. Hanke, R. Thomale, J. Schäfer, and R. Claessen, Bismuthene on a SiC substrate: A candidate for a high-temperature quantum spin Hall material, Science **357**, 287 (2017).

[13] B. Feng, J. Zhang, R.-Y. Liu, T. Iimori, C. Lian, H. Li, L. Chen, K. Wu, S. Meng, F. Komori, and I. Matsuda, Direct evidence of metallic bands in a monolayer boron sheet, Phys. Rev. B **94**, 041408(R) (2016).

[14] B. Feng, O. Sugino, R.-Y. Liu, J. Zhang, R. Yukawa, M. Kawamura, T. Iimori, H. Kim, Y. Hasegawa, H. Li, L. Chen, K. Wu, H. Kumigashira, F. Komori, T.-C. Chiang, S. Meng, and I. Matsuda, Dirac Fermions in Borophene, Phys. Rev. Lett. **118**, 096401 (2017).

[15] B. Feng, J. Zhang, S. Ito, M. Arita, C. Cheng, L. Chen, K. Wu, F. Komori, O. Sugino, K. Miyamoto, T. Okuda, S. Meng, and I. Matsuda, Discovery of 2D Anisotropic Dirac cones, Adv. Mater. **30**, 1704025 (2018).

[16] S. Zhang, Z. Yan, Y. Li, Z. Chen, and H. Zeng, Atomically thin arsenene and antimonene: Semimetal-semiconductor and indirect-direct band-gap transitions, Angew. Chem. **127**, 3155 (2015).

[17] P. Ares, J. J. Palacios, G. Abellán, J. Gómez-Herrero, and F. Zamora, Recent progress on antimonene: A new bidimensional material, Adv. Mater. **30**, 1703771 (2018).

[18] F.-F. Zhu, W.-J. Chen, Y. Xu, C.-L. Gao, D.-D. Guan, C.-H. Liu, D. Qian, S.-C. Zhang, and J.-F. Jia, Epitaxial growth of two-dimensional stanene, Nat. Mater. **14**, 1020 (2015).

[19] C.-C. Liu, H. Jiang, and Y. Yao, Low-energy effective Hamiltonian involving spin-orbit coupling in silicene and two-dimensional germanium and tin, Phys. Rev. B **84**, 195430 (2011).

[20] J. Zegenhagen, E. Fontes, F. Grey, and J. R. Patel, Microscopic structure, discommensurations, and tiling of Si (111)/Cu-"5 × 5," Phys. Rev. B **46**, 1860 (1992).

[21] J. Zegenhagen, P. Lyman, M. Bohringer, and M. Bedzyk, Discommensurate reconstructions of (111) Si and Ge induced by surface alloying with Cu, Ga and In, Phys. Status Solidi B **204**, 587 (1997).

[22] B. Feng, B. Fu, S. Kasamatsu, S. Ito, P. Cheng, C.-C. Liu, Y. Feng, S. Wu, S. K. Mahatha, P. Sheverdyaeva, P. Moras, M. Arita, O. Sugino, T.-C. Chiang, K. Shimada, K. Miyamoto, T. Okuda, K. Wu, L. Chen, Y. Yao, and I. Matsuda, Experimental realization of two-dimensional dirac nodal line fermions in monolayer Cu_2Si, Nat. Commun. **8**, 1007 (2017).

[23] H. Kemmann, F. Müller, and H. Neddermeyer, AES, LEED and TDS studies of Cu on Si(111) 7 × 7 and Si(100) 2 × 1, Surf. Sci. **192**, 11 (1987).

[24] H.-J. Neff, I. Matsuda, M. Hengsberger, F. Baumberger, T. Greber, and J. Osterwalder, High-resolution photoemission study of the discommensurate (5.55 × 5.55) Cu/Si(111) surface layer, Phys. Rev. B **64**, 235415 (2001).

[25] M. D. Santis, M. Muntwiler, J. Osterwalder, G. Rossi, F. Sirotti, A. Stuck, and L. Schlapbach, Electronic and atomic structure of the Cu/Si(111) "quasi-5 × 5" overlayer, Surf. Sci. **477**, 179 (2001).

[26] P. E. Blöchl, Projector augmented-wave method, Phys. Rev. B **50**, 17953 (1994).

[27] G. Kresse and D. Joubert, From ultrasoft pseudopotentials to the projector augmented-wave method, Phys. Rev. B **59**, 1758 (1999).

[28] G. Kresse and J. Hafner, Ab initio molecular dynamics for liquid metals, Phys. Rev. B **47**, 558 (1993).

[29] G. Kresse and J. Hafner, Ab initio molecular-dynamics simulation of the liquid-metal–amorphous-semiconductor transition in germanium, Phys. Rev. B **49**, 14251 (1994).

[30] G. Kresse and J. Furthmüller, Efficiency of ab-initio total energy calculations for metals and semiconductors using a plane-wave basis set, Comput. Mater. Sci. **6**, 15 (1996).

[31] G. Kresse and J. Furthmüller, Efficient iterative schemes for ab initio total-energy calculations using a plane-wave basis set, Phys. Rev. B **54**, 11169 (1996).

[32] I. V. Solovyev, P. H. Dederichs, and V. I. Anisimov, Corrected atomic limit in the local-density approximation and the electronic structure of *d* impurities in Rb, Phys. Rev. B **50**, 16861 (1994).

[33] L.-M. Yang, V. Bačić, I. A. Popov, A. I. Boldyrev, T. Heine, T. Frauenheim, and E. Ganz, Two-dimensional Cu_2Si monolayer with planar hexacoordinate copper and silicon bonding, J. Am. Chem. Soc. **137**, 2757 (2015).

[34] *Silicon (Si), band structure: Datasheet from Landolt-Börnstein — Group III Condensed Matter Volume 41A1β: "Group IV Elements, IV-IV and III-V Compounds. Part b - Electronic, Transport, Optical and Other Properties,"* edited by O. Madelung, U. Rössler, and M. Schulz (Springer-Verlag, Berlin/Heidelberg, 2002).

[35] S. N. Takeda, N. Higashi, and H. Daimon, Visualization of In-Plane Dispersion of Hole Subbands by Photoelectron Spectroscopy, Phys. Rev. Lett. **94**, 037401 (2005).